



STRUCTURAL DAMAGE DETECTION USING A NEW ENHANCED HILBERT-HUANG TRANSFORM METHOD

O. Bahar¹ and S. Ramezani²

ABSTRACT

Recently a new enhanced Hilbert-Huang transform (EHHT) is proposed by the authors, in which the mathematical limitations of the classical Hilbert-Huang transform (HHT) in Hilbert spectral analysis are circumvented. This paper compares performance of the classic and enhanced methods in damage detection of a 7-story reinforced concrete frame during the 1994 Northridge earthquake. In two cases, HHT and EHHT are applied by two different damage detection methods based on Hilbert-Huang approach proposed in literature. In the first and second cases, damage detection based on tracking changes in phase and frequency properties of recorded structural earthquake responses respectively. Results demonstrate that the EHHT offers more advantages than the HHT in both cases.

Introduction

Identification of damages has been an attractive subject for researchers in the field of civil engineering during last decade. Lots of damage detection methods employ signal processing techniques to examine changes in structural properties by tracking the changes in phase and frequency properties in recorded response of the structure.

Hilbert-Huang Transform (HHT) method developed by Huang et al. (1998) is one of the most powerful signal processing methods for analyzing nonstationary and nonlinear signals. Recently, based on this method a few damage detection methods are proposed (*e.g.* Yang et al. 2004, Salvino et al. 2005 and Yinfeng et al. 2008). HHT includes two parts; the empirical mode decomposition (EMD) and the Hilbert spectral analysis (HSA). There are two mathematical theorems that limit the application of HSA. Recently, a new enhanced Hilbert-Huang transform (EHHT) is proposed by the authors, in which mentioned limitations are circumvented (Bahar and Ramezani 2009, Ramezani 2009).

This paper compares the performance of HHT and EHHT in damage detection of a 7-story RC frame building during the 1994 Northridge earthquake. In two cases, HHT and EHHT are applied by two different damage detection methods based on Hilbert-Huang approach proposed in literature. Identification of damage is performed in the first case by tracking phase properties and in the second one by tracking frequency properties. Before the comparison, brief descriptions of the classic and enhanced HHT methods are presented in the following sections.

¹ Assist. Prof., Structural Eng. Dept., International Institute of Earthquake Engineering and Seismology (IIEES), Tehran, Iran

² MSc Graduate in Earthquake Engineering, Structural Eng. Dept., IIEES, Tehran, Iran

The classic Hilbert-Huang transform and its limitations in Hilbert spectral analysis

The HHT includes two parts; the EMD and the HSA. The goal of the EMD as a key part is decomposition of a signal into finite number of intrinsic mode functions (IMFs) with well-behaved Hilbert transform (Huang et al. 1998). The goal of the HSA is calculation of instantaneous frequency and instantaneous amplitude of each IMF through the Hilbert transform.

Empirical mode decomposition

EMD is an algorithm without any analytical definition. EMD decomposes a signal into a finite number of oscillatory modes which called intrinsic mode functions (IMFs). By definition, an IMF is any function that satisfies two conditions: (1) in the whole data set, the number of extrema and the number of zero crossings must either equal or differ at most by one; and (2) at any point, the mean value of the envelope defined by the local maxima and the envelope defined by the local minima is zero. Using this procedure a given signal, $x(t)$, can be decomposed as follows:

$$x(t) = \sum_{i=1}^n c_i(t) + r_n(t) \quad (1)$$

Hilbert spectral analysis

As mentioned above, using HSA instantaneous frequency and instantaneous amplitude of each IMF through the Hilbert transform is calculated. For any real valued function $c(t)$ and its Hilbert transform $y(t)$, the analytic signal, $z(t)$, is defined as:

$$z(t) = c(t) + i y(t) = A(t) e^{i\theta(t)} \quad (2)$$

in which

$$A(t) = \sqrt{c^2(t) + y^2(t)} \quad , \quad \theta(t) = \arctan\left(\frac{y(t)}{c(t)}\right) \quad (3)$$

where $A(t)$ and $\theta(t)$ stand for instantaneous amplitude (envelope) and phase function, respectively. Instantaneous frequency is defined as derivative of the phase function:

$$f(t) = \frac{1}{2\pi} \frac{d\theta(t)}{dt} \quad (4)$$

Therefore, $c(t)$ can be written as:

$$c(t) = \Re(z(t)) = \Re(A(t)e^{i\theta(t)}) = A(t) \cos\theta(t) \quad (5)$$

in which $\Re(\cdot)$ indicates the real part of a complex number. It is clear that, based on the HSA, $c(t)$ and its corresponding Hilbert transform, $y(t)$, have been defined as $A(t)\cos\theta(t)$ and $A(t)\sin\theta(t)$, respectively. $A(t)$ is a positive-valued function and $\theta(t)$ is a monotone increasing function. If $c(t)$ represents an IMF, $x(t)$ can be expressed as the following form:

$$x(t) = \Re \left\{ \sum_{j=1}^n A_j(t) e^{i \int 2\pi f_j(t) dt} \right\} \quad (6)$$

This is a general time-frequency representation of instantaneous amplitude of a signal, which is called the Hilbert spectrum, $H(f, t)$.

Limitations of the Hilbert spectral analysis

EMD procedure fulfills just necessary conditions for applying the HSA, but two unsatisfied requirements according to Bedrosian and Nuttall theorems still exist (Huang and Bethesda 2005). The Bedrosian theorem states that the Hilbert transform of a production of two functions; $A(t)$ and $\cos\theta(t)$, can be written as:

$$H[A(t)\cos\theta(t)] = A(t)H[\cos\theta(t)] \quad (7)$$

only if the Fourier spectra of $A(t)$ and $\cos\theta(t)$ are totally disjointed in frequency space, and if the frequency content of the spectrum of $\cos\theta(t)$ is higher than that of $A(t)$. On the other hand, Nuttall theorem states that if $\theta(t)$ is not a narrow band function but arbitrary function, $H[\cos\theta(t)]$ will not be necessarily $\sin\theta(t)$. To satisfy the requirements of Bedrosian theorem, Huang and Bethesda (2005) proposed the normalized amplitude Hilbert transform (NAHT).

Even if this method performs perfectly, the requirements of Nuttall theorem are not still fulfilled. Huang (2005) have proposed arc-cosine function as an alternative for Hilbert transform to calculate the phase function to satisfy the requirement of Nuttall theorem, but due to imperfect normalization in NAHT method, carrier wave can take values out of $[-1,1]$, therefore the arc-cosine function cannot be correctly applied.

The enhanced Hilbert-Huang transform

In this section, to overcome the mentioned problems an enhanced HHT (EHHT) method is presented (Bahar and Ramezani 2009, Ramezani 2009). In EHHT method, Hilbert transform is replaced by a new procedure based on arc-cosine function, but an IMF is still considered as $A(t)\cos\theta(t)$. The EHHT is summarized in five steps as follows:

1) Perform the EMD to extract IMFs from the signal. For each IMF calculate the instantaneous amplitude, $A(t)$, based on the NAHT method (Huang and Bethesda 2005).

2) For each IMF, normalize positive values by cubic spline interpolant through the local maxima and normalize negative values by absolute value of cubic spline interpolant through the local minima to get the imperfect carrier wave. Determine perfect carrier wave by correcting the positive and negative values of the imperfect carrier wave applying *upper and lower corrective curves*. Upper (lower) corrective curve is defined as a piecewise cubic polynomials which runs through the local maxima (minima) of the imperfect carrier wave with zero slope. Proposed correction is so infinitesimal that cannot affect the imperfect carrier wave considerably.

3) Apply arc-cosine to the perfect carrier wave to determine the phase function, $\theta(t)$, as a monotone increasing function free of the limitation of the Nuttall theorem. According to the definition, instantaneous frequency of an IMF can be achieved by calculating derivative of the

phase function. But in most discrete cases, a noise contaminated phase function results in a physically meaningless frequency with a large dispersion.

4) Define a *cubic smoothing spline* function through the discrete noise contaminated phase functions as follows:

$$S(p) = p \sum_i w_i [y_i - C(x_i)]^2 + (1-p) \int \lambda(z) C''(z)^2 dz \quad (8)$$

where (x_i, y_i) is a set of knots, *i.e.* phase data, $C(x)$ is a cubic spline interpolant function, p is the smoothing parameter, w is a discrete uniform weighting vector and λ is a continuous uniform weighting function. In this study, the value of the uniform vector and function are assumed to be 1, and variation of p is examined. The basic interval of p is $[0,1]$. Very often, the range of interest for p is $p_h = 1/(1+h^3/6)$, where h is the average space between the x_i s. By applying $S(p)$ to the monotone increasing phase function, a smoothed phase function is obtained. Note that, smaller values of p results in a more smoothed phase function with less scattered frequency.

$$f_s(t) = \frac{1}{2\pi} \frac{d\theta_s(t)}{dt} \quad (9)$$

(5) Having instantaneous frequency and instantaneous amplitude for each IMF, enhanced spectrum of the signal, $E(f, p, t)$, can be achieved.

Damage detection of the Van Nuys Hotel building during the 1994 Northridge earthquake

In order to identify the location of damages on a typical building, which has experienced strong ground motions two procedures proposed in the literature are employed. The first procedure is performed based on the proposed method by Salvino et al. (2005) and for the second procedure the method proposed by Yinfeng et al. (2008) is carried out.

The typical building is the Van Nuys Hotel building that was strongly shaken and damaged in the 1971 San Fernando and 1994 Northridge earthquakes. It is a 7-story hotel located in California's San Fernando Valley, Fig. 1. The plan configurations are the same for all the floors and the structural system includes reinforced concrete moment-frames. The building was instrumented under the Strong Motion Instrumentation Program of the California Division of Mines and Geology (CDMG). The location and orientation of the sensors are shown in Fig. 2. Trifunac et al. (1999) have reported the damage of the building during the 1994 Northridge earthquake event; severely wide shear cracks occurred at the middle columns of the exterior south frame on the 5th floor. For uniformity in both procedures, the relative angular accelerations that are defined by Yinfeng et al. (2008) are determined and used to specify the location of damages in the height of the building. The relative angular acceleration a_{i-j} is defined by $a_{i-j} = (a_i - a_j)/d_{i-j}$, where a_i and a_j stand for the accelerations of the sensors reported in nodes i and j , respectively and d_{i-j} is the vertical distance of the nodes. Four relative angular accelerations are determined and shown in Figure ; a_{9-10} , a_{10-11} , a_{11-12} , a_{12-16} . As it can be seen in Figure , the major part of the signals energy is concentrated in the first 20 seconds. As a result, only the first 20 s of the relative angular accelerations are analyzed.



Figure 1. North and south views of the Van Nuys building

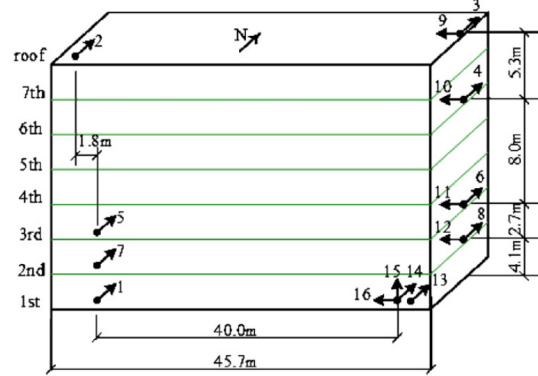


Figure 2. The location and orientation of the sensors in the building (adopted from Yinfeng et al. 2008)

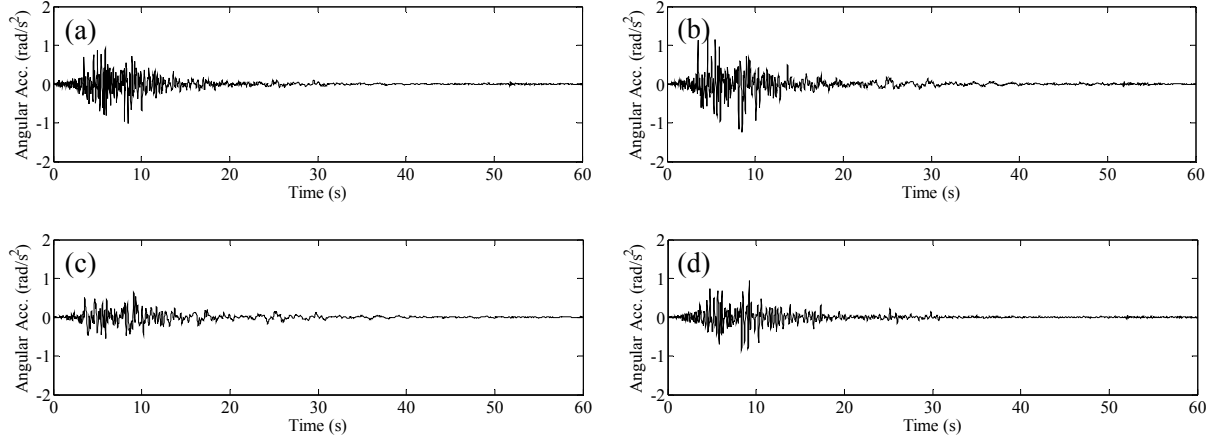


Figure 3. Relative angular accelerations of the Van Nuys Hotel building during the 1994 Northridge earthquake: (a) a_{9-10} , (b) a_{10-11} , (c) a_{11-12} , and (d) a_{12-16}

Damage detection based on tracking phase properties

Based on concept of phase dereverberation, Salvino et al. (2005) have proposed a damage detection method that determines the location of the damage by tracking phase properties between successive degrees of freedom. They defined a total phase function, $\theta_H(t)$, as Eq. 11 which represent the total number of rotations of the signal $x(t)$ in the complex plane for a unique time value t (multiplied by 2π).

$$\theta_H(t) = \sum_{k=1}^n \arctan \left\{ \frac{H[c_k(t)]}{c_k(t)} \right\} \quad (10)$$

in which $c_k(t)$ is the k th IMF and $H[c_k(t)]$ is its corresponding Hilbert transform. Salvino et al. (2005) have shown that lag in $\theta_H(t)$ obtained from measured response can be directly associated with stiffness loss of the structure due to damage. For more details, readers may refer to Salvino et al. (2005).

Using the EHHT, the total phase function can be redefined as $\theta_A(t)$ in the following form:

$$\theta_A(t) = \sum_{k=1}^n \arccos \{CCW_k\} \quad (11)$$

in which CCW_k is the corrected carrier wave corresponding to the k th IMF. $\theta_H(t)$ and $\theta_A(t)$ obtained from the relative angular accelerations are shown in Figs. 4 and 5.

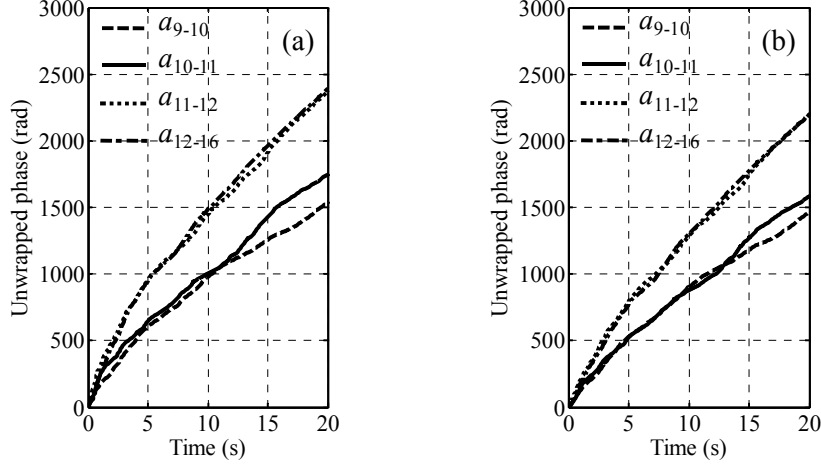


Figure 4. The total phase functions corresponding to the relative angular acceleration by using:
(a) $\theta_H(t)$ from HHT method, and (b) $\theta_A(t)$ from EHHT method

In Fig. 4(a) and (b), the phase lag due to damage shows up in a_{9-10} and a_{10-11} only, indicating the structural damage is located in the distance between sensors 10 and 11. To highlight differences, $\theta_H(t)$ and $\theta_A(t)$ obtained from each relative angular acceleration are presented in Fig. 5. A similar trend in both total phases can be seen for each relative angular acceleration which shows the mentioned limitations for applying HSA do not considerably affect the total phase. But, the inherent end-effect error in the Hilbert transform is magnified by unwrapping and causes $\theta_H(t)$ to be slightly placed upper than $\theta_A(t)$. It can be demonstrated that the EHHT is effectively capable to decrease the end-effect error in determination of both phase and frequency (Ramezani 2009).

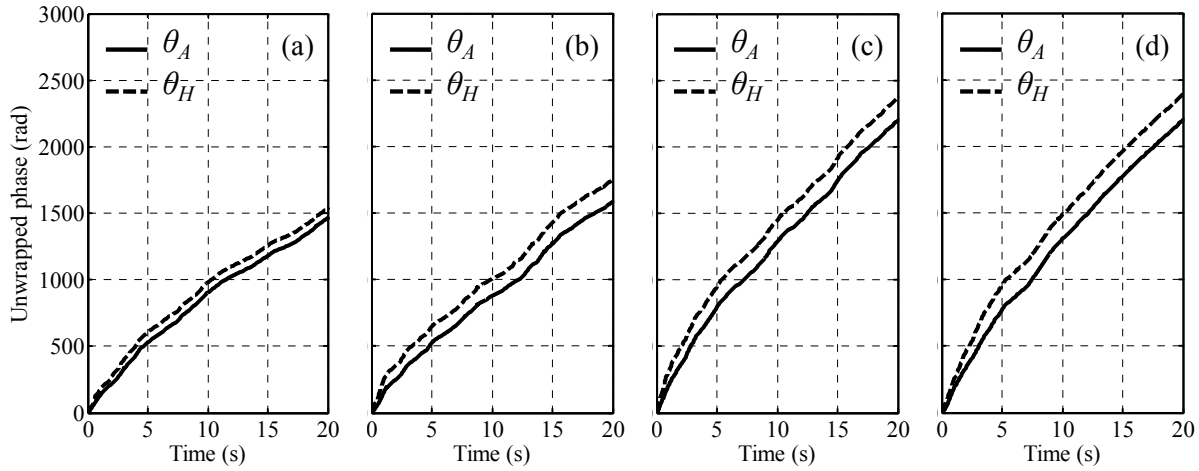


Figure 5. The total phases determined by $\theta_H(t)$ and $\theta_A(t)$ for: (a) a_{9-10} , (b) a_{10-11} , (c) a_{11-12} , and (d) a_{12-16}

Damage detection based on tracking frequency properties

To get an idea of the time-frequency characteristics of the relative angular accelerations, spectra obtained by using the HHT and EHHT are presented in Figs. (6) to (9). Hot colors in all figures indicate the energy concentration of signals. It seems frequency changes of the building started about second 5 and continued until second 10. But, the information as shown in Figs. (6) and (7) are not so clear to understand more. Readability of the spectra in these figures is deteriorated due to wide frequency band of a few first IMFs (Flandrin et al. 2004). EHHT can increase the readability of the spectrum remarkably by adjusting the smoothing parameter as shown in Figs. (8) and (9), in which the amplitude distribution is completely clear.

Clearance of figures using EHHT with lower smoothing parameter makes it possible considering the amplitude changes of IMFs. It can be seen in Fig. (8) that the trend of IMFs in (c) and (d) are very similar but completely different with (a) and (b). This can be explained by stiffness loss of the building due to damage occurred in the floors between sensors 10 and 11 about second 5. Another change is obvious around second 10, but our information is not such complete that we can explain the event.

Yinfeng et al. (2008) have defined the instantaneous average frequency (IAF) as the first order moment of the squared time varying spectrum with respect to frequency as $IAF(t) = \sum_{i=1}^n [A_i^2(t)f_i(t)] / \sum_{i=1}^n [A_i^2(t)]$ where $A_i(t)$ and $f_i(t)$ denote the instantaneous amplitude and frequency of the i th IMF, respectively. IAF's obtained by using HHT and EHHT corresponding to the relative angular accelerations are shown in Fig. 10. IAFs in Fig. 10(a) and (b) are quite similar and it is obvious that IAF of a_{10-11} is placed below the other IAFs for most of the time caused by damaged in structure. Smoother IAFs can be achieved through the EHHT by decreasing the smoothing parameter as done in Fig. 10(c) and (d) in which variation of resulting IAF's is clearer.

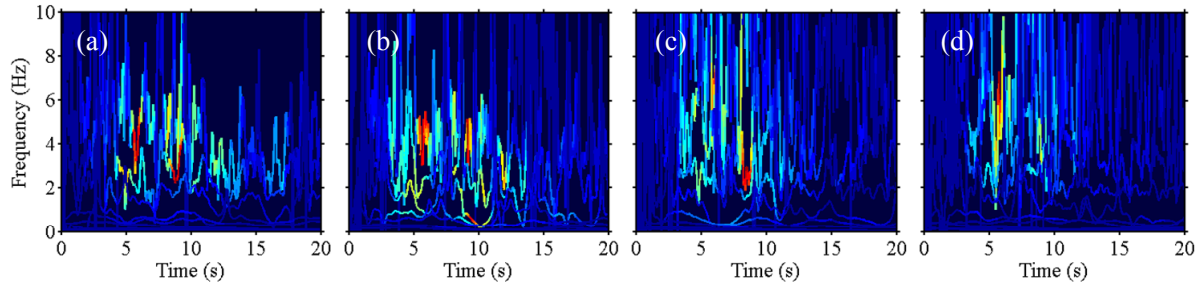


Figure 6. Spectra using the HHT: (a) a_{9-10} , (b) a_{10-11} , (c) a_{11-12} , and (d) a_{12-16}

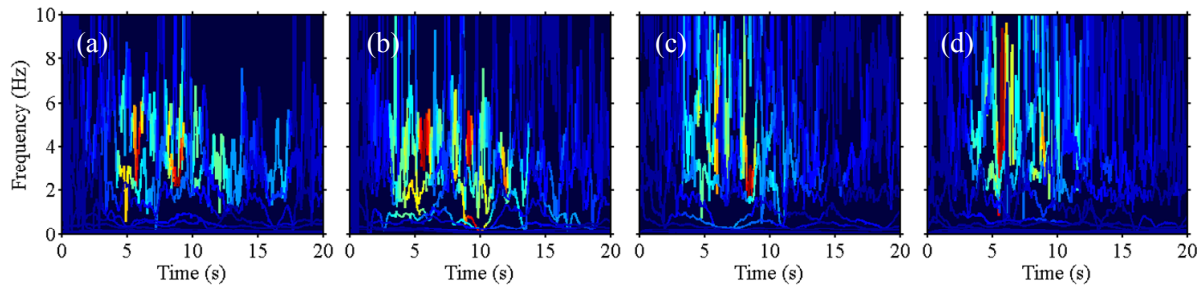


Figure 7. Spectra using the EHHT, $p = p_h$: (a) a_{9-10} , (b) a_{10-11} , (c) a_{11-12} , and (d) a_{12-16}

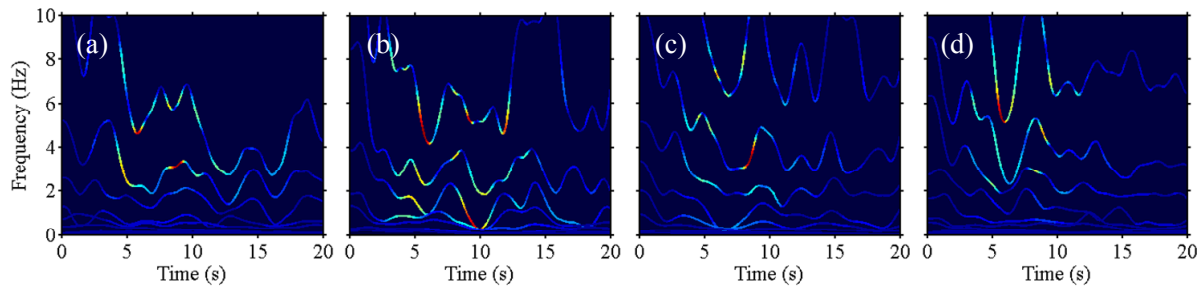


Figure 8. Spectra using the EHHT, $p = 0.50$: (a) a_{9-10} , (b) a_{10-11} , (c) a_{11-12} , and (d) a_{12-16}

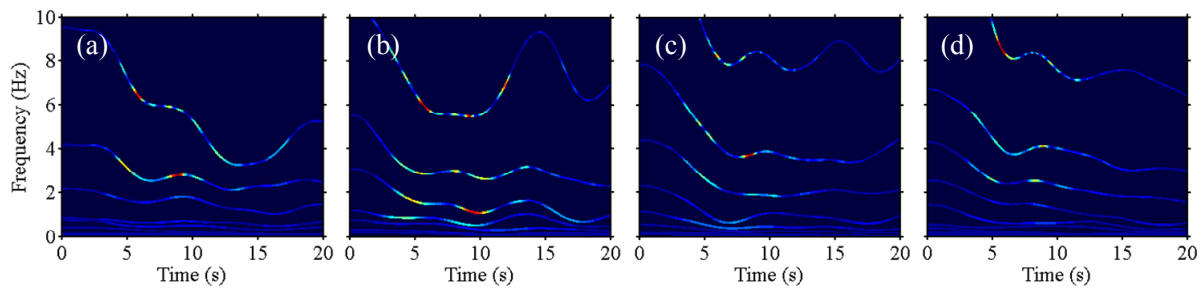


Figure 9. Spectra using the EHHT, $p = 0.01$: (a) a_{9-10} , (b) a_{10-11} , (c) a_{11-12} , and (d) a_{12-16}

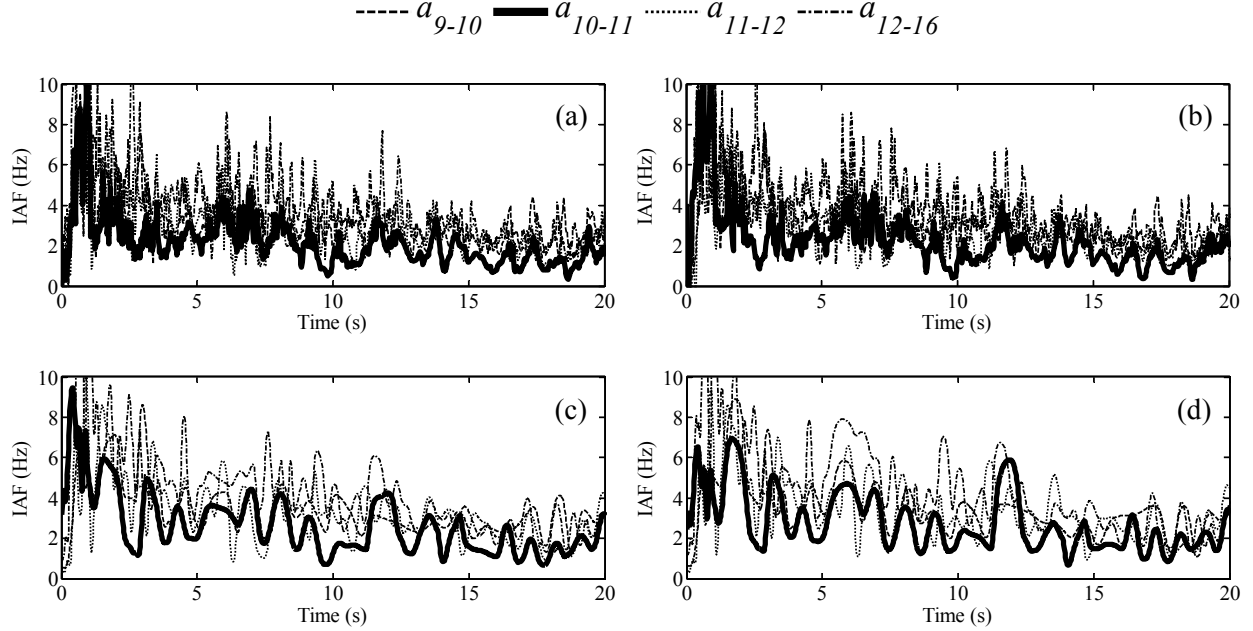


Figure 10. IAF's obtained by using: (a) HHT, (b) EHHT, $p = p_h$, (c) EHHT, $p = 0.99$ (d) EHHT, $p = 0.50$ and (e) EHHT, $p = 0.01$

Conclusions

The classical Hilbert-Huang transform and its limitations in Hilbert spectral analysis briefly reviewed. A new enhanced Hilbert-Huang transform (EHHT) has been recently proposed by authors is explained, in which the limitations of the Hilbert spectral analysis are circumvented. Using two different procedures, performance of the HHT and EHHT are compared in damage detection of a 7-story RC building (the Van Nuys Hotel Building) during the 1994 Northridge earthquake. Two different damage detection methods based on the Hilbert-Huang approach have been proposed in the literature. In the first procedure, damage was detected based on tracking changes in phase properties of recorded structural responses in which EHHT yielded more advantages in accurate determination of the phase function than the HHT. In the second procedure, damage was detected by tracking changes in frequency properties of the recorded structural responses. In the latter procedure, the EHHT offers more meaningful results than the HHT in determination and tracking of the frequency. The results show that EHHT method is a powerful tool for researching in the field of structural damage detection.

References

Bahar O., Ramezani S., 2009, Analysis of non stationary and nonlinear signals using a new enhanced Hilbert-Huang Transform, *Signal processing* (submitted).

Flandrin, P., Rilling, G., and Goncalves, P., 2004. Empirical mode decomposition as a filter bank, *IEEE Signal Proc Let* 11, 112–114.

Huang, N. E., Shen, Z., Long, S.R., Wu, M. C., Shin, H. S., Zheng, Q., et al., 1998. The empirical mode decomposition and the Hilbert spectrum for nonlinear and non-stationary time series analysis, *Proc.*

R. Soc. London 454, 903–995.

Huang, N. E., 2005. Introduction to Hilbert-Huang transform and some recent developments, in: Huang N. E., and Attoh-Okine, N. O., Eds., *The Hilbert-Huang Transform in Engineering*, Taylor & Francis, Boca Raton.

Huang, N. E., and Bethesda, M. D., 2005. Computing instantaneous frequency by normalizing Hilbert transform, *US Patent* 6901353.

Ramezani S., 2009. “Developing a system identification method based on a new enhanced Hilbert-Huang transform”, *MSc thesis*, International Institute of Earthquake Engineering and Seismology, Tehran.

Salvino, L., Pines, D. J., Tod, M., and Nichols, J., 2005, EMD and instantaneous phase detection of structural damage, in: Huang, N. E., and Shen, S., Eds., *Hilbert-Huang Transform and its applications*, World Scientific, Singapore.

Trifunac, M. D., Ivanovic, S. S., Todorovska, M. I., 1999. Instrumented 7-storey reinforced concrete building in Van Nuys, California: description of damage from the 1994 Northridge earthquake and strong motion data, *USC Report CE* 99-02.

Yang, J. N., Lei, Y., Lin, S., and Huang, N. E., 2004. Hilbert-Huang Based Approach for Structural Damage Detection, *Journal of Engineering Mechanics* 130, 85–95.

Yinfeng, D., Yingmin, L., Mingkui X., and Ming, L., 2008. Analysis of earthquake ground motions using an improved Hilbert-Huang transform, *Soil Dynamic and Earthquake Engineering* 28, 7–19.